Resource Allocation in Energy-Cooperation Enabled Two-Tier NOMA HetNets Toward Green 5G

Bingyu Xu, Yue Chen, *Senior Member, IEEE*, Jesús Requena Carrión, *Member, IEEE*, and Tiankui Zhang, *Senior Member, IEEE*

***Abstract*— This paper focuses on resource allocation in energy-cooperation enabled two-tier heterogeneous networks (HetNets) with non-orthogonal multiple access (NOMA), where base stations (BSs) are powered by both renewable energy sources and the conventional grid. Each BS can serve multiple users at the same time and frequency band. To deal with the fluctuation of renewable energy harvesting, we consider that renewable energy can be shared between BSs via the smart grid. In such networks, user association and power control need to be re-designed, since existing approaches are based on OMA. Therefore, we formulate a problem to find the optimum user association and power control schemes for maximizing the energy efficiency of the overall network, under quality-of-service constraints. To deal with this problem, we first propose a distributed algorithm to provide the optimal user association solution for the fixed transmit power. Furthermore, a joint user association and power control optimization algorithm is developed to determine the traffic load in energy-cooperation enabled NOMA HetNets, which achieves much higher energy efficiency performance than existing schemes. Our simulation results demonstrate the effectiveness of the proposed algorithm, and show that NOMA can achieve higher energy efficiency performance than OMA in the considered networks.**

***Index Terms*— Non-orthogonal multiple access (NOMA), HetNets, energy cooperation, user association, power control.**

I. Introduction

IN FIFTH generation (5G) mobile systems, one main goal is to improve energy efficiency significantly compared to today's networks [1]. However, triggered by the proliferation of mobile internet services and Internet of things (IoT), a large number of devices will be connected in future wireless networks [2]. Indeed, such large level of connectivity will inevitably give rise to an unprecedented surge in global energy consumption. The latest analysis shows that the energy demand for information and communications technology already accounts for almost 10% of the world's total energy consumption [3]. In addition, critical environmental issues such as high carbon emissions are a big concern. Hence, "greener" solutions need to be developed to enhance the network energy efficiency. Among the emerging technologies, energy harvesting is regarded as one viable solution [4]. By allowing base stations (BSs) to harvest energy from renewable energy sources such as solar and wind, the conventional grid energy consumption of wireless networks can be greatly reduced. Moreover, energy cooperation between BSs via the smart grid can further improve the utilization of renewable energy [5].

Manuscript received January 27, 2017; revised May 15, 2017; accepted May 23, 2017. Date of publication July 12, 2017; date of current version December 22, 2017. *(Corresponding author: Bingyu Xu.)*

B. Xu, Y. Chen, and J. R. Carrión are with the School of Electronic Engineering and Computer Science, Queen Mary University of London, London E1 4NS, U.K. (e-mail: bingyu.xu@qmul.ac.uk; yue.chen@qmul.ac.uk; j.requena@qmul.ac.uk).

T. Zhang is with the School of Information and Communication Engineering, Beijing University of Posts and Telecommunications, Beijing 100876, China (e-mail: zhangtiankui@bupt.edu.cn).

Color versions of one or more of the figures in this paper are available online at http://ieeexplore.ieee.org.

Digital Object Identifier 10.1109/JSAC.2017.2726398

A. Prior Works and Motivation

Although renewable energy harvesting is a viable solution for cutting the conventional grid energy consumption in cellular networks, there exist many challenges for integrating energy harvesting capabilities into BSs [6]. In renewable energy harvesting enabled networks, BSs will harvest variable amounts of renewable energy, due to the fluctuating nature of renewable energy sources. When the renewable energy harvested by BSs is insufficient to meet their load conditions, some user equipments (UEs) have to be offloaded to distant BSs with abundant energy and may suffer more from signal degradation. Moreover, some BSs may always have excessive harvested energy (e.g., because of more favorable whether conditions) that will eventually be wasted. Since the deployment of BSs with large energy storage capabilities brings high expenditure of networks [7], the energy fluctuation problem cannot be solely solved by using storage. To tackle this problem, energy cooperation is introduced as a means for harvested renewable energy to be shared between BSs during the energy transmission process [8].

Energy cooperation in the point-to-point transmission scenario has been studied in [5], [8], and [9]. In [9], one-way energy transfer in the Gaussian two-way channel and multiple access channel were considered respectively. This line of work was extended to the two-way case in [5]. The implementation of energy cooperation in multiple access channels and multiple access relay networks were studied in [10] and [11], respectively. In [12], an energy cooperation scheme in cognitive radio networks was proposed to improve both the spectral and energy efficiency.

Recently, the potential of energy cooperation in renewable energy enabled cellular networks has been explored, and various energy-cooperation optimization problems have been studied. In [7], a joint energy and spectrum allocation problem between two neighboring cellular systems was formulated, which aimed to minimize the cost of energy and bandwidth, and the problem was solved by convex optimization. The power control problem between two BSs was considered

in [13] under the assumption that the harvested energy and the energy demand of BSs were deterministic. In [14], the energy cost of cellular networks was minimized with the assumption that BSs traded energy via the smart grid with different prices. The work of [15] aimed to maximize the sum rate through optimizing the transmit powers of BSs in a coordinated multipoint cluster. In [16], the energy trading problem was formulated to minimize the average cost of energy exchange between BSs, and a dynamic algorithm was proposed based on the Lyapunov optimization technique, which did not require the statistical knowledge of the channel and energy.

While the aforementioned studies have laid a solid foundation for understanding energy cooperation in renewable energy enabled networks, existing contributions only have paid attention to energy cooperation in orthogonal multiple access (OMA) cellular networks. To the best of our knowledge, research on energy cooperation in non-orthogonal multiple access (NOMA) cellular networks has not been conducted.

Multiple access in wireless networks is a technique that allows multiple users to share available resources such as time and spectrum based on a specific scheme [17]. System performance can be improved by selecting the multiple access technology appropriately. In general, there are two types of multiple access schemes, namely OMA and NOMA [18]. In OMA systems such as time division multiple access (TDMA), and orthogonal frequency-division multiple access (OFDMA), time and spectrum resources are allocated orthogonally so as to eliminate the interference among users. The rationale of NOMA is to exploit the power or code domain in order to save time and frequency resources [18]–[21]. Compared to OMA, NOMA allows BSs to serve multiple users simultaneously in the same frequency band and can substantially enhance the spectral efficiency. In this paper, we focus on NOMA in the power domain. In power domain NOMA, power allocation plays a crucial role for the overall system performance. In [22], the energy efficiency in a downlink cell with one BS and multiple users was maximized. An energy efficiency optimization problem in a multiple-input multiple-output (MIMO) network with one BS was formulated in [19]. Based on the observation that user's quality of service (QoS) in NOMA systems is an important performance indicator, a dynamic power control scheme in both downlink and uplink NOMA scenarios was proposed in [23], where the average rate and outage probability constraints were considered. In [24], two power control optimization problems were formulated to minimize the transmit power and maximize the rate fairness, respectively.

Besides the power allocation problem, existing works such as [25]–[27] also focused on the joint subchannel assignment and power control design in NOMA systems. A joint subchannel assignment and power allocation optimization problem was formulated in [25] to maximize the energy efficiency of the overall network. In [26], a joint power control and subcarrier allocation problem was studied to minimize the overall transmit power. In [27], a suboptimal scheme was proposed to provide a good solution for maximizing the overall throughput in the multi-carrier NOMA system with a single BS.

Although intensive research has been conducted on the design of NOMA transmission, resource allocation in NOMA multi-cell networks remains an open problem. Considering the fact that user association (UA) determines that users should be connected to a specified BS to form a user group for superposition transmission [28], the number of users associated with a BS can have a significant effect on the spectral and energy efficiency in NOMA multi-cell networks. In addition, power control is of great importance in such networks, since the intra-cell interference and inter-cell interference need to be coordinated. Otherwise the performance of cell edge users will be significantly degraded [29].

B. Contributions and Organization

While there are many previous studies considering resource allocation in conventional energy-cooperation enabled OMA cellular networks, the resource allocation problem in energy-cooperation enabled NOMA multi-cell networks has not been addressed, specifically for UA and power control. Meanwhile, most of existing NOMA works such as [22]–[27] only consider the case consisting of one BS and a group of users. The effect of inter-cell interference in practical multi-cell scenarios is not considered, despite the fact that it has a substantial impact on the system performance. Although UA and power control have been studied in conventional OMA cellular networks such as [30] and [31] and in single-cell NOMA networks such as [32], existing designs are unsuitable for multi-cell NOMA networks because multi-cell NOMA transmission characteristics are not considered. Moreover, current research on UA with renewable energy harvesting such as [33] and [34] only focuses on OMA networks without energy cooperation. In particular, [33], [34] studied how UA can be designed to cut the energy consumption of the network. To date, UA and power control solutions in multi-cell NOMA networks have not been studied. Motivated by this, in this paper, we study the power control and UA problem in energy-cooperation enabled two-tier NOMA HetNets. The main contributions of this paper are summarized as follows:

- We consider the downlink transmissions in energy-cooperation enabled two-tier NOMA HetNets, where a high-power macro BS is underlaid with a group of pico BSs and renewable energy can be shared between BSs. In such networks, each BS is powered by both renewable energy sources and the conventional power grid. A resource allocation problem is formulated for optimizing the UA, transmit power, transferred energy between BSs and grid energy consumption, which aims to maximize the energy efficiency of the overall network while ensuring the QoS of users.
- We first study UA under fixed transmit powers. A distributed algorithm is proposed to find an efficient UA solution based on the Lagrangian dual analysis, which outperforms its conventional counterpart and a genetic-algorithm (GA) based UA with fixed population size. Then, a joint UA and power control algorithm is proposed to further maximize the energy efficiency. The performance of the proposed algorithm is compared with different conventional schemes, including the

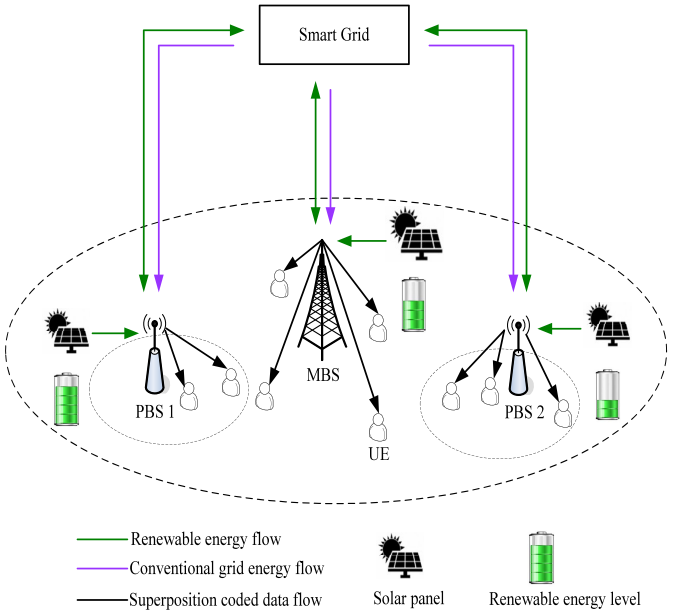

Fig. 1. An example of an energy-cooperation enabled two-tier NOMA HetNet powered by both solar panels and the conventional grid.

fractional transmission power allocation (FTPA), and the cases without renewable energy or energy cooperation respectively.

- Our results confirm that the proposed algorithm can achieve much higher energy efficiency than the conventional schemes. The proposed power control can well coordinate the intra-cell and inter-cell interference, compared to the existing ones. Moreover, our algorithm can achieve larger multiuser diversity gains and BS densification gains.

The remainder of the paper is organized as follows: Section II presents the system model and the formulated problem. Section III describes the proposed resource allocation algorithm under the fixed transmit power. After that, the resource allocation scheme under the fixed UA scheme and the proposed joint UA and power control algorithm are presented in Section IV. Finally, Section V and VI provide simulation results and the conclusion respectively.

II. Network Model and Problem Formulation

In this section, the system model for energy cooperation in two-tier NOMA HetNets is presented, and the corresponding joint UA and power control problem is formulated.

A. Downlink NOMA Transmission

As shown in Fig. 1, we consider a two-tier energy-cooperation enabled HetNet consisting of one macro BS (MBS) and M pico BSs (PBSs), where NOMA-based downlink transmission is utilized, and all BSs are assumed to share the same frequency band. In such a network, BSs are powered by both the conventional power grid and renewable energy sources, and energy can be shared between BSs through the smart grid. Let $m \in \{1, 2, 3, \ldots, M+1\}$ be the m-th BS, in which $m = 1$ denotes the MBS, and the other values denote PBSs. There are N randomly located user equipments (UEs) in this network, and each UE is associated with only one BS. All BSs and UEs are single-antenna nodes. In this paper, it is assumed that the global perfect channel state information (CSI) is available. Let $j \in \{1, 2, 3, \ldots, N\}$ index the j-th UE. According to the NOMA scheme [19], [21], the superimposed signal transmitted by the BS m is $s_m = \sum_{j=1}^{N} x_{jm}\sqrt{P_{jm}}s_{jm}$ with $\mathrm{E}\left[s_{jm}\left(s_{jm}\right)^H\right] = 1$, $\forall m, j$, where $x_{jm} \in \{0, 1\}$ is the binary UA indicator, i.e., $x_{jm} = 1$ when the j-th UE is associated with the m-th BS and otherwise it is zero, s_{jm} is the j-th user-stream and P_{jm} is the corresponding allocated transmit power. When the j-th UE is associated with the m-th BS, its received signal can be expressed as

$$y_{jm} = h_{jm}\sqrt{P_{jm}}s_{jm} + \underbrace{h_{jm}\sum_{j^{'}=1, j^{'}\neq j}^{N} x_{j^{'}m}\sqrt{P_{j^{'}m}}s_{j^{'}m}}_{\text{Intra-cell interference}} + \underbrace{\sum_{m^{'}=1, m^{'}\neq m}^{M+1} h_{jm}^{m^{'}}\left(\sum_{j^{'}=1}^{N} x_{j^{'}m^{'}}\sqrt{P_{j^{'}m^{'}}}s_{j^{'}m^{'}}\right)}_{\text{Inter-cell interference}} + \varpi_o, \quad (1)$$

where $x_{j^{'}m}, x_{j^{'}m^{'}} \in \{0, 1\}$, h_{jm} is the channel coefficient from the associated BS m, $h_{jm}^{m^{'}}$ is the interfering channel coefficient from the BS $m^{'}$, and ϖ_o is the additive white Gaussian noise. The power density of ϖ_o is σ^2. In NOMA systems, successive interference cancelation (SIC) is employed at UEs, to cancel the intra-cell interference from the stronger UEs' data signals. Without loss of generality, assuming that there are k_m ($k_m \leq N$) UEs constituting a group that is served by the m-th BS at the same time and frequency band, the corresponding channel to inter-cell interference plus noise ratios (CINRs) are ordered as

$$\frac{|h_{1m}|^2}{I_{1m}^{(2)} + \sigma^2} \geq \cdots \geq \frac{|h_{jm}|^2}{I_{jm}^{(2)} + \sigma^2} \geq \cdots \geq \frac{|h_{k_m m}|^2}{I_{k_m m}^{(2)} + \sigma^2}, \quad (2)$$

where $I_{jm}^{(2)}$ is the inter-cell interference power at the j-th UE and σ^2 is the noise power. Based on the principle of multi-cell NOMA [19], the power allocation of the users' data signals in the m-th cell needs to satisfy

$$0 \leq P_{1m} \leq \cdots \leq P_{jm} \leq \cdots \leq P_{k_m m}, \quad \sum_{j=1}^{k_m} P_{jm} = P_m, \quad (3)$$

where P_m is the total transmit power of the m-th BS. Such order is optimal for decoding and guarantees the user fairness [19], namely the data signals of users with weaker downlink channels and larger interference need to be allocated more transmit power to achieve the desired QoS. For the special case of single-cell, i.e., $I_{jm}^{(2)} = 0$, (3) reduces to the order based on the channel power gains, as seen in [21]. Therefore, based on (1), the data rate after SIC at the j-th UE is given by

$$\tau_{jm} = W \log_2\left(1 + \gamma_{jm}\right), \quad (4)$$

where W is the system bandwidth, and γ_{jm} is the signal-to-interference-plus-noise ratio (SINR) given by

$$\gamma_{jm} = \frac{P_{jm}\left|h_{jm}\right|^2}{\underbrace{\left|h_{jm}\right|^2\sum_{j'=1}^{j-1}P_{j'm}}_{I_{jm}^{(1)}} + \underbrace{\sum_{m'=1,m'\neq m}^{M+1}\left|h_{jm}^{m'}\right|^2 P_{m'}}_{I_{jm}^{(2)}} + \sigma^2} = \frac{P_{jm}}{\sum_{j'=1}^{j-1}P_{j'm} + (I_{jm}^{(2)}+\sigma^2)/\left|h_{jm}\right|^2}, \quad j \le k_m \tag{5}$$

in which $I_{jm}^{(1)}$ is the remaining intra-cell interference after SIC, and $P_{m'} = \sum_{j'=1}^{N} x_{j'm'}P_{j'm'}$ is the total transmit power of the m'-th BS. Although this paper focuses on the single-carrier system, it can be straightforwardly extended to the multi-carrier system by letting W be the subcarrier bandwidth and τ_{jm} multiply the subcarrier indicator to be the data rate of a subcarrier. Thus, the optimal solution over all subcarriers in the multi-carrier case can be iteratively obtained by following the decomposition approach of this paper.

B. Energy Model

Each BS is powered by both the conventional grid and renewable energy sources. The energy drawn by the m-th BS from the conventional grid is denoted as G_m. The energy harvested by the m-th BS from renewable energy sources is denoted by E_m. The energy transferred from BS m to BS m' is denoted as $\mathcal{E}_{mm'}$, and the energy transfer efficiency factor between two BSs is denoted as $\beta_{\mathcal{E}} \in [0,1]$. Hence $(1-\beta_{\mathcal{E}})$ specifies the level of energy loss during the energy transmission process. In addition, we assume that there is no battery to avoid the time-consuming and expensive energy waste during the charging/discharging process, and the energy-cooperation problem in each time slot is independent. We normalize the time slot length as one to simplify the power-to-energy conversion. Therefore, the transmit energy consumption at the m-th BS should satisfy

$$P_m \le G_m + E_m + \underbrace{\beta_{\mathcal{E}}\sum_{m'=1,m'\neq m}^{M+1}\mathcal{E}_{m'm}}_{\text{Energy received from other BSs}} - \underbrace{\sum_{m'=1,m'\neq m}^{M+1}\mathcal{E}_{mm'}}_{\text{Energy transferred to other BSs}}, \tag{6}$$

where $P_m = \sum_{j=1}^{N} x_{jm}P_{jm}$ is the total transmit power of the m-th BS.

From (6), we see that in energy-cooperation enabled networks, the grid energy consumption of a BS depends on its harvested renewable energy, transferred energy and transmit power. Given a BS's transmit power, its grid energy consumption needs to be formulated as a random variable, since the amount of harvested renewable energy and transferred energy is uncertain, which is different from the conventional network without energy cooperation.

C. Problem Formulation

Our aim is to maximize the energy efficiency of such networks. The energy efficiency (bits/Joule) is defined as the ratio of the overall network data rate to the overall grid energy consumption, i.e., the network utility is

$$\mathcal{U}(\mathbf{x},\mathbf{P},\boldsymbol{\mathcal{E}},\mathbf{G}) = \Big(\sum_{m=1}^{M+1}\sum_{j=1}^{N}x_{jm}\tau_{jm}\Big)\Big/\sum_{m=1}^{M+1}G_m. \tag{7}$$

In this way, the harvested renewable energy can be maximally utilized to reduce the grid energy consumption [4]. Therefore, our problem can be formulated as

$$\begin{aligned}
\mathbf{P1}: \max_{\mathbf{x},\mathbf{P},\boldsymbol{\mathcal{E}},\mathbf{G}} \ & \mathcal{U}(\mathbf{x},\mathbf{P},\boldsymbol{\mathcal{E}},\mathbf{G}) \\
\text{s.t. C1}: \ & \sum_{m=1}^{M+1}x_{jm}\tau_{jm} \ge \overline{\tau}_{\min}, \quad \forall j, \\
\text{C2}: \ & \sum_{m=1}^{M+1}x_{jm} = 1, \quad \forall j, \\
\text{C3}: \ & P_m + \sum_{m'=1,m'\neq m}^{M+1}\mathcal{E}_{mm'} \le G_m + E_m + \beta_{\mathcal{E}}\sum_{m'=1,m'\neq m}^{M+1}\mathcal{E}_{m'm}, \quad \forall m, \\
\text{C4}: \ & \sum_{j=1}^{N}x_{jm}P_{jm} = P_m, \quad \forall m, \\
\text{C5}: \ & x_{jm}\in\{0,1\}, \quad \forall j,\forall m, \\
\text{C6}: \ & G_m \ge 0, \mathcal{E}_{mm'} \ge 0, \quad \forall j, \ \forall m, \\
\text{C7}: \ & 0 \le P_m \le P_{\max}^m, P_{jm} \ge 0, \quad \forall j, \ \forall m,
\end{aligned} \tag{8}$$

where $\mathbf{x} = [x_{jm}]$, $\mathbf{P} = [P_{jm}]$, $\boldsymbol{\mathcal{E}} = [\mathcal{E}_{mm'}]$, $\mathbf{G} = [G_m]$, $\overline{\tau}_{\min}$ denotes the required minimum data rate for a UE, $P_{\max}^m$ is the maximum transmit power of the BS m. Constraint C1 guarantees the QoS. C2 and C5 ensure that each UE cannot be associated with multiple BSs. C3 is the energy consumption constraint and C4 is the power allocation under NOMA principle in a cell. C6 indicates that the consumed grid energy and transferred energy are non-negative values, and C7 is the maximum transmit power constraint.

From the objective of **P1** and its constraint C3, we find that when more renewable energy is harvested and shared between BSs, the total grid energy consumption of the network can be reduced, which boosts the energy efficiency.

III. Resource Allocation Under Fixed Transmit Power

P1 is a mixed integer non-linear programming (MINLP) problem, and constitutes a challenging problem. In this section,

we assume that the transmit power is fixed, and accordingly the original problem **P1** can be simplified as

$$\mathbf{P2}: \max_{\mathbf{x},\boldsymbol{\mathcal{E}},\mathbf{G}} \mathcal{U}(\mathbf{x},\boldsymbol{\mathcal{E}},\mathbf{G}) \quad \text{s.t. C1, C2, C3, C4, C5, C6.} \tag{9}$$

The problem **P2** is still a combinatorial problem due to its discrete nature. To efficiently solve it, we adopt a decomposition approach. For a given $\mathbf{G}$ and $\boldsymbol{\mathcal{E}}$, the above problem can be rewritten as

$$\mathbf{P2.1}: \max_{\mathbf{x}} \mathcal{U}(\mathbf{x}) \quad \text{s.t. C1, C2, C4, C5.} \tag{10}$$

A. Lagrangian Dual Analysis

Based on **P2.1**, the Lagrangian function can be written as

$$L(\mathbf{x},\boldsymbol{\lambda},\boldsymbol{\theta}) = \mathcal{U}(\mathbf{x}) - \sum_{j=1}^{N}\lambda_j\left(\overline{\tau}_{\min} - \sum_{m=1}^{M+1} x_{jm}\tau_{jm}\right) - \sum_{m=1}^{M+1}\theta_m\left(\sum_{j=1}^{N} x_{jm}P_{jm} - P_m\right), \tag{11}$$

where λ_j and θ_m are the non-negative Lagrange multipliers. Then, the dual function is given by

$$g(\boldsymbol{\lambda},\boldsymbol{\theta}) = \begin{cases} \max\limits_{\mathbf{x}} \; L(\mathbf{x},\boldsymbol{\lambda},\boldsymbol{\theta}) \\ \text{s.t. C2, C5,} \end{cases} \tag{12}$$

and the dual problem of **P2.1** is expressed as

$$\min_{\boldsymbol{\lambda},\boldsymbol{\theta}} g(\boldsymbol{\lambda},\boldsymbol{\theta}). \tag{13}$$

Given the dual variables λ_j and θ_m, the optimal solution for maximizing the Lagrangian w.r.t. $\mathbf{x}$ is

$$x_{jm}^{*} = \begin{cases} 1, & \text{if } \; m = m^{*} \\ 0, & \text{otherwise,} \end{cases} \tag{14}$$

where $m^{*} = \underset{m}{\text{argmax}}\left(\mu_{jm}\right)$ with

$$\mu_{jm} = \tau_{jm}/\sum_{m=1}^{M+1} G_m + \lambda_j\tau_{jm} - \theta_m P_{jm}. \tag{15}$$

The solution of (14) can be intuitively interpreted based on the fact that given the grid energy consumption, users select BSs which provide the maximum data rates. Since the objective of the dual problem is not differentiable, we utilize the subgradient method to obtain the optimal solution $(\boldsymbol{\lambda}^{*},\boldsymbol{\theta}^{*})$ of the dual problem, which is given by

$$\lambda_j(t+1) = \left[\lambda_j(t) - \delta(t)\left(\sum_{m=1}^{M+1} x_{jm}\tau_{jm} - \overline{\tau}_{\min}\right)\right]^{+}, \tag{16}$$

$$\theta_m(t+1) = \left[\theta_m(t) - \delta(t)\left(P_m - \sum_{j=1}^{N} x_{jm}P_{jm}\right)\right]^{+}, \tag{17}$$

where $[a]^{+} = \max\{a, 0\}$, t is the iteration index, and $\delta(t)$ is the step size. Note that there exist several step size selections such as constant step size and diminishing step size. Here, we use the nonsummable diminishing step length [37].

After obtaining the optimal $(\boldsymbol{\lambda}^{*},\boldsymbol{\theta}^{*})$ based on (16) and (17), the corresponding $\mathbf{x}$ is the solution of the primal problem **P2.1**. Therefore, based on the Lagrangian dual analysis, UA can be determined in a centralized or distributed way. The centralized UA is intuitive, and requires a central controller, which has the global CSI and determines which user is connected to a BS in this network. In this paper, we propose a distributed UA algorithm which does not require any centralized coordination, as summarized in Algorithm 1. Since our problem satisfies the conditions of the convergence proof in [37], the convergence of the proposed algorithm is guaranteed. The complexity of the proposed algorithm is $O((M+1)N)$ for each iteration and the convergence is fast (less than 40 iterations in the simulation), which is much lower than the brute force algorithm $O\left((M+1)^{N}\right)$. Note that the broadcast operations have negligible effect on computational complexity.

B. Genetic Algorithm

In this subsection, we develop a GA-based UA to solve the problem **P2.1**. Such algorithm will be compared with the proposed Algorithm 1. GA can achieve good performance when the population of candidate solutions is sufficient [38]. Specifically, each feasible chromosome represents a possible solution that satisfies the constraints of problem **P2.1**, which

Algorithm 1 Distributed User Association

Step 1: At user side

1: **if** $t = 0$
2: Initialize $\lambda_j(t)$, $\forall j$. Each UE measures its received inter-cell interference via pilot signal from all BSs, and feedbacks the CINR values to the corresponding BSs. Meanwhile, each UE selects the BS with the largest CINR value.
3: **else**
4: User j receives the values of μ_{jm} and τ_{jm} from BSs.
5: Determines the serving BS m according to $m^{*} = \underset{m}{\text{argmax}}\left(\mu_{jm}\right)$.
6: Update $\lambda_j(t)$ according to (16).
7: **end if**
8: $t \leftarrow t+1$.
9: Each user feedbacks the UA request to the chosen BS, and broadcasts the value of $\lambda_j(t)$.

Step 2: At BS side

1: **if** $t = 0$
2: Initialize $\theta_m(t)$, $\forall m$.
3: **else**
4: Receives the updated user association matrix $\mathbf{x}$.
6: Updates $\theta_m(t)$ according to (17), respectively.
7: Each BS calculates μ_{jm} and τ_{jm} under NOMA principle.
8: **end if**
9: $t \leftarrow t+1$.
10: Each BS broadcasts the values of μ_{jm} and τ_{jm}.

is defined as

$$\mathcal{D}_i = \{[m_{1i}], [m_{2i}], \ldots, [m_{Ni}]\},\ i \in \{1, \ldots, K\}, \quad (18)$$

where m_{ji} is the gene representing the index of the BS that the j-th UE is associated with, and it has an integer value varying from 1 to $M+1$, and K is the population size. During each generation, the fitness of each chromosome is evaluated, to select high fitness chromosomes and produce higher fitness offsprings. Based on the objective of problem **P2.1**, the fitness value of the chromosome $\mathcal{D}_i$ is calculated as

$$\Phi_i(\mathcal{D}_i) = \mathcal{U}(\mathcal{D}_i). \quad (19)$$

Then, all chromosomes are ranked from the best to the worst with ranking r, based on their fitness values. The probability that a chromosome is selected as a parent to produce offspring is given by $\rho_s(r) = \frac{q(1-q)^{r-1}}{1-(1-q)^K}$ with a predefined value q [38]. In each generation process, a uniform crossover operation with the probability ρ_c is utilized to produce offspring by swapping and recombining genes based on the parental chromosomes. In addition, a uniform mutation operation with the probability ρ_m is employed. Such generation procedure is repeated until reaching the maximum number of generations, and is summarized in Algorithm 2. Given the maximum number of generations Ω and fixed population size K, the complexity of the proposed algorithm is $O(\Omega K \log(K))$ [39]. The performance of the GA-based UA algorithm heavily depends on the population size and number of generations, due to the inherent nature of GA [38]. In the simulation results of Section V, we will demonstrate that overall, the proposed Algorithm 1 outperforms GA-based Algorithm 2 when the population size of GA is not very large, and thus has lower complexity.

Algorithm 2 Genetic Algorithm-Based User Association Algorithm

1: **if** $t = 0$
2: Initialize a set of feasible chromosomes $\{\mathcal{D}_i\}$ with population size K, and the maximum number of generations $t_{\max}$.
3: **else**
4: Rank $\{\mathcal{D}_i\}$ based on the fitness values given by (19).
5: Based on the selection probability $\rho_s(r)$, chromosomes are selected to produce offspring via uniform crossover and mutation operations.
6: **if** exceed the maximum number of generations
7: $x^*_{jm} := \{\mathcal{D}^*_i\}$, where $\{\mathcal{D}^*_i\}$ is the feasible chromosome with the highest fitness value.
8: **break**
9: **else**
10: $t \leftarrow t + 1$.
11: **end if**
12: **end if**

The aforementioned approach provides UA solutions for problem **P2.1**. After obtaining the UA solution $\mathbf{x} = \left[x^*_{jm}\right]$, the corresponding pair $(\mathbf{G}, \boldsymbol{\mathcal{E}})$ is obtained by solving the following simple linear programming (LP):

$$\mathbf{P2.2}: \min_{\boldsymbol{\mathcal{E}}, \mathbf{G}} \sum_{m=1}^{M+1} G_m \quad \text{s.t. C3, C6.} \quad (20)$$

The problem **P2.2** can be efficiently solved by using existing software, e.g. CVX [40].

When no energy cooperation is allowed, i.e., $\mathcal{E}_{mm'} = 0$, $\forall j, \forall m$, the optimal grid energy consumption $\mathbf{G}$ of problem **P2.2** under the UA solution $\mathbf{x} = \left[x^*_{jm}\right]$ is directly obtained as

$$G^*_m = [P_m - E_m]^+, \quad (21)$$

where $P_m = \sum_{j=1}^{N} x^*_{jm} P_{jm}$.

Based on the solutions of subproblems **P2.1** and **P2.2**, we propose an iterative algorithm to solve the problem **P2**, which is summarized in Algorithm 3.

Algorithm 3 Resource Allocation Algorithm Under Fixed Transmit Power

1: **if** $t = 0$
2: For a fixed $\mathbf{P}$, initialize $G_m, \forall j, m$.
3: **else**
4: Determine $x_{jm}(t)$ under fixed $(\boldsymbol{\mathcal{E}}, \mathbf{G})$ by selecting the user association algorithm from Algorithm 1 or Algorithm 2.
5: Given $x_{jm}(t)$, update the energy allocation policy $(\boldsymbol{\mathcal{E}}, \mathbf{G})$ by solving the LP **P2.2** via CVX.
6: **if** convergence
7: Obtain optimal resource allocation policy $(\mathbf{x}^*, \boldsymbol{\mathcal{E}}^*, \mathbf{G}^*)$.
8: **break**
9: **else**
10: $t \leftarrow t + 1$.
11: **end if**
12: **end if**

IV. Resource Allocation Under Power Control

In this section, we consider the joint resource allocation and power control design. Specifically, we develop an algorithm to solve the MINLP problem **P1** through the decomposition approach. As discussed in the previous section, we first determine the UA indicators given the resource allocation policy $(\mathbf{P}, \boldsymbol{\mathcal{E}}, \mathbf{G})$, which can be obtained by solving problem **P2.1** via Algorithm 1 or Algorithm 2. Then, under a fixed UA $\{x_{jm}\}$, the problem for optimizing $(\mathbf{P}, \boldsymbol{\mathcal{E}}, \mathbf{G})$ is written as

$$\mathbf{P3}: \max_{\mathbf{P}, \boldsymbol{\mathcal{E}}, \mathbf{G}} \mathcal{U}(\mathbf{P}, \boldsymbol{\mathcal{E}}, \mathbf{G}) \quad \text{s.t. C1, C3, C4, C6, C7.} \quad (22)$$

From the utility function, we find that the power allocation vectors $\mathbf{P}$ and $\mathbf{G}$ are coupled in the objective of problem **P3**. Thus, given $\mathbf{G}$ and $\boldsymbol{\mathcal{E}}$, the above problem can be decomposed into

$$\mathbf{P3.1}: \max_{\mathbf{P}} \sum_{m=1}^{M+1} \sum_{j=1}^{N} x_{jm} \tau_{jm} \quad \text{s.t. C1, C3, C4, C7.} \quad (23)$$

Problem **P3.1** is non-convex. Hence we provide a tractable suboptimal solution based on the Karush-Kuhn-Tucker (KKT) conditions. The Lagrangian function of problem **P3.1** is

$$L(\mathbf{P}, \boldsymbol{\nu}, \boldsymbol{\chi}) = \sum_{m=1}^{M+1}\sum_{j=1}^{N} x_{jm}\tau_{jm} - \sum_{j=1}^{N+1}\chi_j\Big(\overline{\tau}_{\min} - \sum_{m=1}^{M+1} x_{jm}\tau_{jm}\Big) - \sum_{m=1}^{M+1}\nu_m\Big(\sum_{j=1}^{N} x_{jm}P_{jm} - \varphi_m\Big), \quad (24)$$

where $\varphi_m = \min\Big\{G_m + E_m + \beta_{\mathcal{E}}\sum_{m'=1,m'\neq m}^{M+1}\mathcal{E}_{m'm} - \sum_{m'=1,m'\neq m}^{M+1}\mathcal{E}_{mm'}, P_{\max}^{m}\Big\}$ according to constraints C3 and C7, and χ_j and ν_m are the non-negative Lagrange multipliers.

Without loss of generality, assuming that the j-th UE is associated with the BS m, i.e., $x_{jm} = 1$, based on the KKT conditions, we have

$$\frac{\partial L}{\partial P_{jm}} = (1+\chi_j)\left(\frac{W\Lambda_{jm}}{1+P_{jm}\Lambda_{jm}}\right) - \Theta_{jm}^{(1)} - \Theta_{jm}^{(2)} - \nu_m\log(2) = 0, \quad (25)$$

where $\Lambda_{jm} = \frac{|h_{jm}|^2}{I_{jm}^{(1)}+I_{jm}^{(2)}+\sigma^2}$ is referred to as the channel to interference plus noise ratio at the j-th UE. Based on (3) and (5), $\Theta_{jm}^{(1)}$ resulting from the intra-cell interference is given by

$$\Theta_{jm}^{(1)} = \sum_{\ell>j}^{k_m}(1+\chi_\ell)\,\frac{W\gamma_{\ell m}}{1+\gamma_{\ell m}}\Lambda_{lm}, \quad (26)$$

and $\Theta_{jm}^{(2)}$ resulting from the inter-cell interference is given by

$$\Theta_{jm}^{(2)} = \sum_{m'=1,m'\neq m}^{M+1}\sum_{j'=1}^{N}\frac{\left(1+\chi_{j'}\right)x_{j'm'}W\gamma_{j'm'}\left|h_{j'm'}^{m}\right|^2}{\left(1+\gamma_{j'm'}\right)\left(I_{j'm'}^{(1)}+I_{j'm'}^{(2)}+\sigma^2\right)}. \quad (27)$$

Based on (25), the transmit power allocated to the j-th user-stream in the m-th cell is obtained as

$$P_{jm}^{*} = \Big[\frac{(1+\chi_j)W}{\Theta_{jm}^{(1)}+\Theta_{jm}^{(2)}+\nu_m\log(2)} - \frac{1}{\Lambda_{jm}}\Big]^{+}. \quad (28)$$

In (28), the allocated transmit power is a monotonic function of ν_m. As such, given $\{\chi_j\}$, we adopt a one-dimension search over the Lagrange multipliers $\{\nu_m\}$, which can efficiently obtain the optimal $\boldsymbol{\nu}^*$ that satisfies constraints C3 and C7. According to (28), we can easily find that ν_m^* needs to satisfy $0 \le \nu_m^* \le \nu_m^{\max}$, where $\nu_m^{\max} = \max_j\Big\{\Big((1+\chi_j)W\Lambda_{jm} - \Theta_{jm}^{(1)} - \Theta_{jm}^{(2)}\Big)/\log(2)\Big\}$. Here, $\nu_m^* = 0$ represents that there is no limitation about the transmit power of the j-th user-stream and $\nu_m^* = \nu_m^{\max}$ corresponds to the case that no transmit power is allocated to the j-th user-stream. Thus, by fixing $\{\chi_j\}$, $\boldsymbol{\nu}^*$ can be obtained by using Algorithm 4. For achieving a specific accuracy ς, the complexity of Algorithm 4 is $O(\log(1/\varsigma))$.

Algorithm 4 One-Dimension Search Algorithm

1: **if** $t = 0$
2: Given χ_j, initialize $\nu_m^l = 0, \nu_m^h = \nu_m^{\max}, \forall m$, and calculate $F_l = \sum_{j=1}^{N} x_{jm}P_{jm}^{*(l)}$ and $F_h = \sum_{j=1}^{N} x_{jm}P_{jm}^{*(h)}$, where $\left\{P_{jm}^{*(l)}\right\}$ and $\left\{P_{jm}^{*(h)}\right\}$ are the allocated transmit powers of the j-th UE's data stream for the cases of ν_m^l and ν_m^h respectively, which are calculated by using (28).
3: **else**
4: **while** $F_l \neq \varphi_m$ and $F_h \neq \varphi_m$
5: Let $\nu_m = \frac{\nu_m^l+\nu_m^h}{2}$, and compute F_m.
6: **if** $F_m = \nu_m$
7: The optimal dual variable ν_m^* is obtained.
8: **break**
9: **elseif** $F_m < \varphi_m$
10: $\nu_m^h = \nu_m$.
11: **else** $F_m > \varphi_m$
12: $\nu_m^l = \nu_m$.
13: **end if**
14: **end while**
15: **end if**

After obtaining $\boldsymbol{\nu}^*$, the Lagrange multiplier χ_j can be updated by using the subgradient method, which is similar to (16).

To ensure the system stability, we utilize the Mann iterative method to update the transmit power in each iteration [41], which is given by

$$P_{jm}^{(\ell+1)} = (1-\eta(\ell))P_{jm}^{(\ell)} + \eta(\ell)P_{jm}^{*}, \quad (29)$$

where ℓ is the iteration index, $0 < \eta(\ell) < 1$ is the step size, which is usually chosen as $\eta(\ell) = \frac{\ell}{2\ell+1}$. After obtaining the optimal solution of problem **P3.1**, the corresponding $(\mathbf{G}, \mathbf{\mathcal{E}})$ can be updated by solving the LP problem **P2.2** via CVX. As such, the solution of problem **P3** can be iteratively obtained. Note that the convergence of KKT-based algorithm is usually faster than the gradient-based designs [42].

Based on the previous analysis, the proposed joint UA and power control scheme in energy-cooperation enabled NOMA HetNets is summarized in Algorithm 5.

A. Comparison With FTPA

In 4G networks FTPA scheme is adopted [19]. The rule of FTPA is that the transmit power will be allocated based on the UEs' channel conditions, i.e., the data signals of UEs with weaker downlink channels will own more transmit power. Based on the CINR order in (30), the transmit power allocated to the j-th UE's data stream in the m-th cell under FTPA protocol is expressed as [19]

$$P_{jm} = P_m\left(\frac{|h_{jm}|^2}{I_{jm}^{(2)}+\sigma^2}\right)^{-\alpha} \Big/ \sum_{l=1}^{N} x_{lm}\left(\frac{|h_{lm}|^2}{I_{lm}^{(2)}+\sigma^2}\right)^{-\alpha}, \quad (30)$$

where $0 \le \alpha \le 1$ is the decay factor. Here, $\alpha = 0$ represents equal power allocation. For larger α, the transmit

Algorithm 5 Joint User Association and Power Control

1: **if** $t = 0$
2: Initialize $P_m, G_m, E_m, \forall m$
3: **else**
4: Determine $x_{jm}(t)$ under $(\mathbf{P}, \mathbf{G}, \boldsymbol{\mathcal{E}})$ by selecting the user association algorithm from Algorithm 1 or Algorithm 2.
5: Given $x_{jm}(t)$ and the corresponding $(\mathbf{G}, \boldsymbol{\mathcal{E}})$, update the transmit power $\mathbf{P}$ based on the following rule:
Loop:
a) Given $\Theta_{jm}^{(2)}$, loop over UE j:
i): Obtain $\{\nu_m^*\}$ using Algorithm 4 given $\{\chi_j\}$
ii): Obtain P_{jm} according to (28) with $\{\nu_m^*, \chi_j\}$.
iii): Update $\{\chi_j\}$ using subgradient method.
iv): Update P_{jm} using (29).
Until convergence.
b) Update $\Theta_{jm}^{(2)}$ using (27).
Until convergence.
6: Based on the updated $\mathbf{P}$, update G_m and $\mathcal{E}_{mm'}$ by solving LP problem **P2.2** via CVX.
7: **if** convergence
8: Obtain optimal resource allocation policy $(\mathbf{x}^*, \mathbf{P}^*, \boldsymbol{\mathcal{E}}^*, \mathbf{G}^*)$.
9: **break**
10: **else**
11: $t \leftarrow t + 1$.
12: **end if**
13: **end if**

power allocated to the data-stream of the user with largest CINR becomes lower, and more power will be allocated to the data-stream of the user with the lowest CINR, in order to achieve the user-fairness and the optimal decoding. However, the detrimental effect of using such simple power allocation scheme is that distant users may receive severer inter-cell interference without power control among BSs, due to the fact that each BS has to assign larger transmit power to the far-away users. Therefore, compared to the single-cell NOMA case [21], the inter-cell interference has a significant impact on the power allocation of multi-tier NOMA HetNets.

B. Comparison With No Renewable Energy

When there is no renewable energy harvesting (i.e., $E_m = 0, \ \forall m$), no renewable energy can be shared between BSs (i.e., $\mathcal{E}_{mm'} = \mathcal{E}_{m'm} = 0, \ \forall m, m'$), and thus the required energy can only be supplied by the conventional grid. In this case, $P_m = G_m, \ \forall m$, and the original problem **P1** reduces to

$$\mathbf{P4}: \max_{\mathbf{x},\mathbf{P}} \frac{\sum_{m=1}^{M+1}\sum_{j=1}^{N} x_{jm}\tau_{jm}}{\sum_{m=1}^{M+1}\sum_{j=1}^{N} x_{jm}P_{jm}} \quad \text{s.t. C1, C2, C4, C5, C7.} \tag{31}$$

The above problem is non-linear fractional programming and NP-hard, which can be solved by using the proposed Algorithm 5 with $E_m = 0$ and $\mathcal{E}_{mm'} = \mathcal{E}_{m'm} = 0$.

TABLE I
SIMULATION PARAMETERS

Parameter	Value
System bandwidth	10 MHz
Noise power density	-174 dBm/Hz
Cell radius	500 m
Path loss of MBS	$128.1 + 37.6\log_{10} d(\text{km})$
Path loss of PBS	$140.7 + 36.7\log_{10} d(\text{km})$
Max transmit power of MBS	46 dBm [43]
Max transmit power of PBS	30 dBm [43]

C. Comparison With No Energy Cooperation

In this case, the energy transfer efficiency $\beta_{\mathcal{E}}$ is set to 0, which means that the harvested renewable energy cannot be transferred between BSs. Each BS is powered by the conventional grid and its harvested renewable energy, i.e., the transmit energy consumption at a BS needs to satisfy $P_m \leq G_m + E_m, \ \forall m$. Then, the proposed Algorithm 5 can still be applied to solve this problem, and during each iteration, the grid energy consumption is updated as $G_m = [P_m - E_m]^+$ based on the updated P_m.

V. SIMULATION RESULTS

In this section, we present numerical results to demonstrate the effectiveness of the proposed algorithm compared with other schemes as well as the conventional counterpart. Since the renewable energy arrival rate changes slowly in practice and is stationary at each information transmission time slot [44], we consider the amounts of harvested energy at the MBS and PBSs to be constant and each PBS has the same level of renewable energy during each transmission time slot for the sake of simplicity. Our analysis and proposed algorithm are independent of the specific renewable energy distribution. In the simulation, we focus on the large-scale channel fading condition in low mobility environment, due to the fact that UA is carried out in a large time scale and the small-scale fading can be averaged out [33], [34]. In addition, PBSs and UEs are uniformly distributed in a macrocell geographical area. The basic simulation parameters are shown in Table I.

A. User Association Under Fixed Transmit Power

In this subsection, we study different UA algorithms under fixed transmit power, i.e., power control is unavailable at BSs. Based on the NOMA power allocation condition in (3), we consider that the total transmit power at each BS is $P_m = P_{\max}^m$, and adopt an arithmetic progression power allocation approach for the sake of simplicity, namely the transmit power of the j-th user's data signal is $P_{jm} = \frac{2j}{k_m(1+k_m)} P_m$, $j \in \{1, 2, 3, \ldots, k_m\}$ when k_m users are multiplexed in the power domain of the m-th cell. We also provide the comparison with the conventional Reference Signal Received Power (RSRP) based UA. The aim of this subsection is to show the performance for different UA algorithms under the same fixed power allocation condition.

Fig. 2 shows the energy efficiency versus the number of UEs with the number of PBSs $M = 6$ and the energy transfer efficiency factor $\beta_{\mathcal{E}} = 0.9$. We set the minimum QoS as

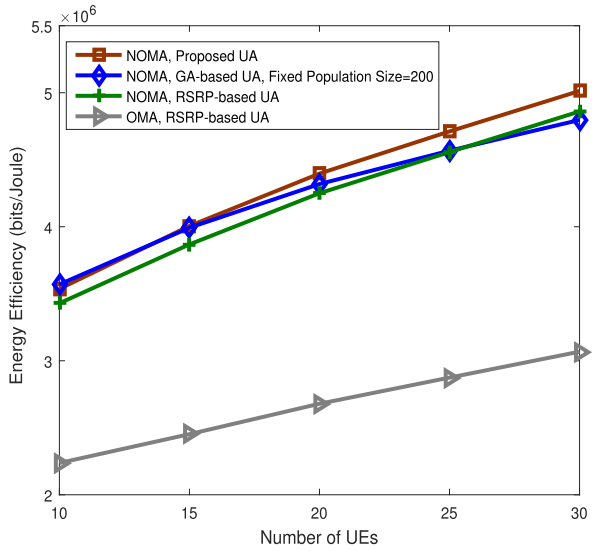

Fig. 2. Energy efficiency versus the number of UEs for different UA algorithms.

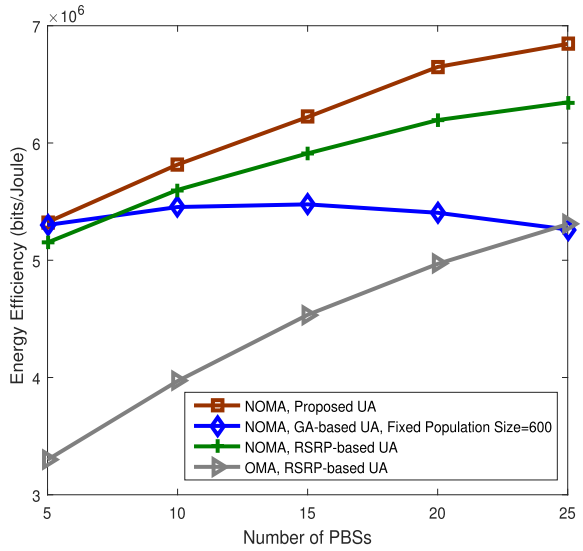

Fig. 3. Energy efficiency versus the number of PBSs for different UA algorithms.

$\overline{\tau}_{\min} = 0.1$ bits/s/Hz and the amount of energy harvested by MBS and PBS as 37 dBm and 27 dBm, respectively.[1] The maximum number of generations for the GA-based UA is 10, $q = 0.1$, and $\rho_c = \rho_m = 0.4$. The proposed UA scheme with NOMA achieves better energy efficiency than the other cases. The energy efficiency increases with the number of UEs because of the multiuser diversity gain (i.e., different users experience different path loss, and more users with lower path loss help enhance the overall energy efficiency.) [35]. The use of NOMA outperforms OMA. By using the GA-based UA, the energy efficiency slowly increases with the number of UEs, due to the fact that the efficiency of the GA-based algorithm depends on the population size [38]. In other words, given the population size (e.g., $K = 200$ in this figure), the GA algorithm may not obtain good solutions when the number of UEs grows large, which indicates that larger populations of candidate solutions is needed [38].

Fig. 3 shows the energy efficiency versus the number of PBSs with the number of UEs $N = 40$ and the energy transfer efficiency factor $\beta_{\mathcal{E}} = 0.9$. We set the minimum QoS as $\overline{\tau}_{\min} = 0.1$ bits/s/Hz and the amount of harvested energy at MBS and PBS as 37 dBm and 27 dBm, respectively. The maximum number of generations for GA is 10, $q = 0.1$, and $\rho_c = \rho_m = 0.4$. NOMA achieves higher energy efficiency than OMA, since NOMA can achieve higher spectral efficiency. The proposed UA algorithm outperforms the other cases, and the performance gap between the proposed UA and the conventional RSRP-based UA is larger when deploying more PBSs, due to the fact that the proposed UA can achieve more BS densification gains [36]. For the GA-based UA algorithm with the population size $K = 600$, solutions are inferior when the number of PBSs is large, as larger populations of candidate solutions are needed [38].

[1]In real networks, the renewable energy generation rate is constant during a certain period, and the time scale of the UA and power control process is much shorter, typically less than several minutes [33], [34]. In addition, the amount of energy harvested by a MBS is usually larger than that at a PBS, since MBS can fit larger solar panel [34], [45].

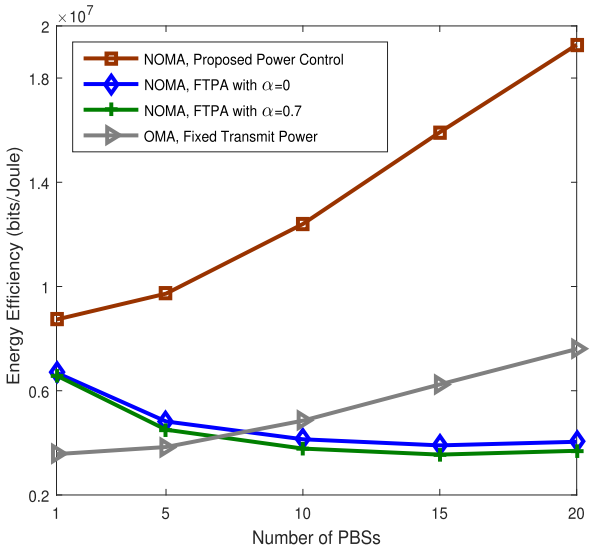

Fig. 4. Energy efficiency versus the number of PBSs for different power allocation policies.

B. Power Control Under Fixed User Association

In this subsection, we consider three power allocation schemes, namely the power control method proposed in Section IV, FTPA and the conventional fixed transmit power, to confirm the advantages of our proposal. We adopt the conventional RSRP-based UA in the simulation, and all the considered cases experience the same UA condition. In addition, BSs use their maximum transmit powers in the OMA scenario, and the total transmit power of each BS for FTPA is set as $P_m = P_{\max}^m$, $m \in \{1, 2, 3, \ldots, M+1\}$.

Fig. 4 shows the energy efficiency versus the number of PBSs with the number of UEs $N = 50$ and the energy transfer efficiency factor $\beta_{\mathcal{E}} = 0.9$. We set the minimum QoS as $\overline{\tau}_{\min} = 1$ bits/s/Hz and the amount of energy harvested by MBS and PBS as 37 dBm and 27 dBm, respectively. We see that by using NOMA with the proposed power control, energy efficiency rapidly increases with the number of PBS.

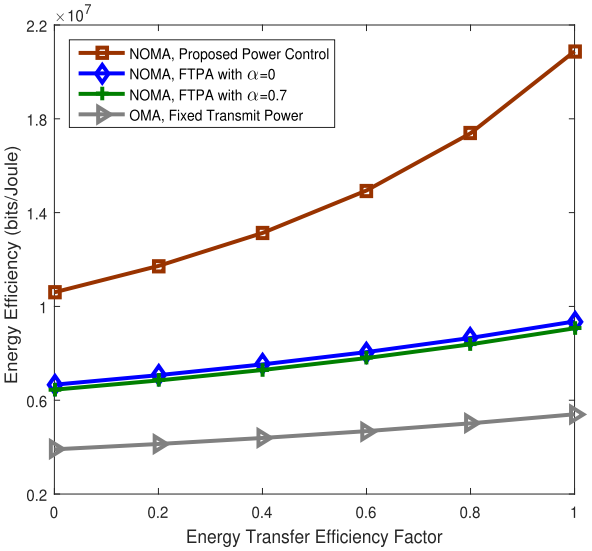

Fig. 5. Energy efficiency versus energy transfer efficiency factor for different power allocation policies.

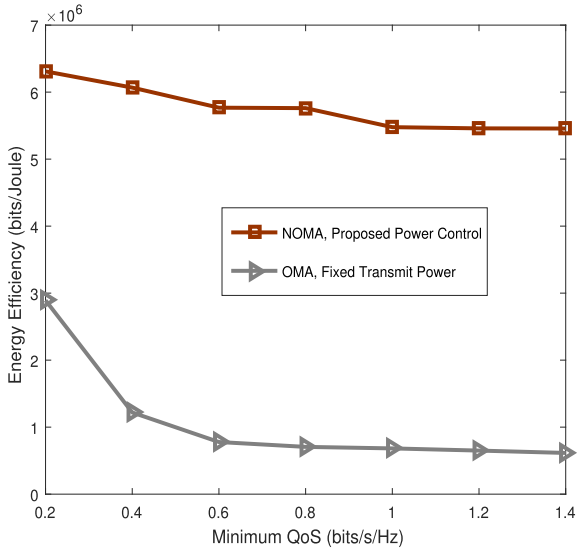

Fig. 6. Tradeoff between the energy efficiency and the minimum QoS for NOMA and OMA.

The proposed algorithm achieves better performance than the other cases. When deploying more PBSs, the performance gap between the proposed solution and the other cases is larger, which indicates that the proposed power control algorithm can achieve more BS densification gains and efficiently coordinate the inter-cell interference. When the number of PBSs is not large, NOMA with FTPA can outperform the conventional OMA case, since NOMA can achieve better spectral efficiency than OMA [21]. However, when adding more PBSs, NOMA with FTPA may not provide higher energy efficiency. The reason is that more UEs will be offloaded to picocells, and the inter-cell interference will become severer, which means that the transmit power of each user-stream needs to be larger to combat the inter-cell interference. As suggested in Section IV-A, FTPA with $\alpha = 0$ achieves higher energy efficiency of the network than the $\alpha = 0.7$ case, since the data-streams for UEs with poorer channel condition (i.e., lower CINR) have to be allocated more power in the case of FTPA with $\alpha = 0.7$, which reduces the total throughput of the network under the same energy consumption.

Fig. 5 shows the energy efficiency versus the energy transfer efficiency factor $\beta_{\mathcal{E}}$ with the number of PBSs $M = 3$ and the number of UEs $N = 40$. We set the minimum QoS to $\overline{\tau}_{\min} = 1$ bits/s/Hz and the amount of harvested energy at MBS and PBS to 40 dBm and 35 dBm, respectively. Compared to the no energy-cooperation case (i.e., $\beta_{\mathcal{E}} = 0$), the use of energy cooperation can enhance the energy efficiency, particularly when the energy transfer efficiency factor is large. The implementation of NOMA can achieve higher energy efficiency than the conventional OMA system because of higher spectral efficiency, and the proposed power control algorithm outperforms the other cases. Moreover, the energy efficiency grows at a much higher speed when applying the proposed algorithm. For a specified $\beta_{\mathcal{E}}$, FTPA with $\alpha = 0$ achieves higher energy efficiency of the network than the $\alpha = 0.7$ case, as suggested in Fig. 4.

Fig. 6 shows the tradeoff between the energy efficiency and the minimum QoS with the number of PBSs $M = 3$ and the number of UEs $N = 30$. We set the energy transfer efficiency factor to $\beta_{\mathcal{E}} = 0.9$ and the amount of energy harvested by MBS and PBS to 37 dBm and 27 dBm, respectively. For a given minimum QoS, the proposed power control under NOMA achieves higher energy efficiency than conventional OMA. When better QoS is required by the UE, energy efficiency of both NOMA and OMA cases decreases. The reason is that for the proposed solution, more transmit power will be allocated to the UEs with lower CINRs to achieve such minimum QoS, which results in more energy consumption; for conventional OMA, it means that more users cannot obtain the desired QoS and have to experience outage. We see that energy efficiency decreases significantly in the low minimum QoS regime, because many UEs receive low QoS and increasing the level of the minimum QoS means that these UEs cannot be served. In practice, the minimum QoS can be found in an off-line manner [46].

C. Joint User Association and Power Control

In this subsection, we examine the benefits of joint UA and power control design in energy-cooperation enabled NOMA HetNets. We also present comparisons by considering different power allocation schemes with the conventional RSRP-based UA. In the OMA scenario, transmit power at the BS is set to $P_m = P_{\max}^m$ in the OMA scenario.

Fig. 7 shows the energy efficiency versus the number of UEs with the number of PBSs $M = 5$ and the energy transfer efficiency factor $\beta_{\mathcal{E}} = 0.9$. We set the minimum QoS as $\overline{\tau}_{\min} = 0.5$ bits/s/Hz and the amount of harvested energy at MBS and PBS as 32 dBm and 22 dBm, respectively. We see that the proposed joint UA and power control algorithm achieves higher energy efficiency than the other cases, and significantly improves the performance when more UEs are served in the network. The reason is that the proposed algorithm is capable of obtaining larger multiuser diversity gains. The use of NOMA can obtain higher energy efficiency than the OMA case, due to NOMA's capability of achieving

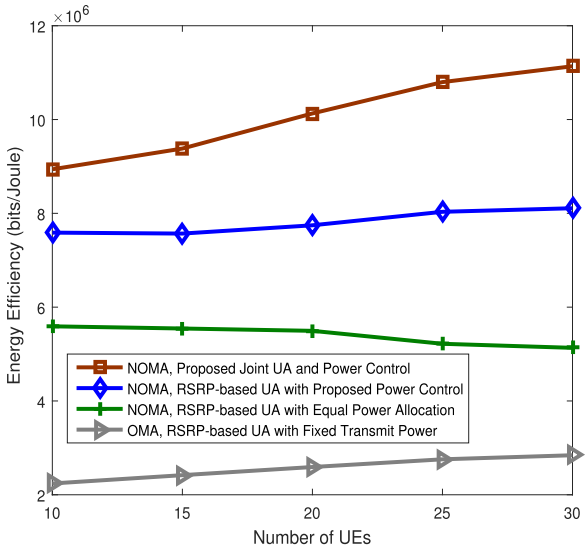

Fig. 7. Energy efficiency versus the number of UEs for different joint UA and power allocation designs.

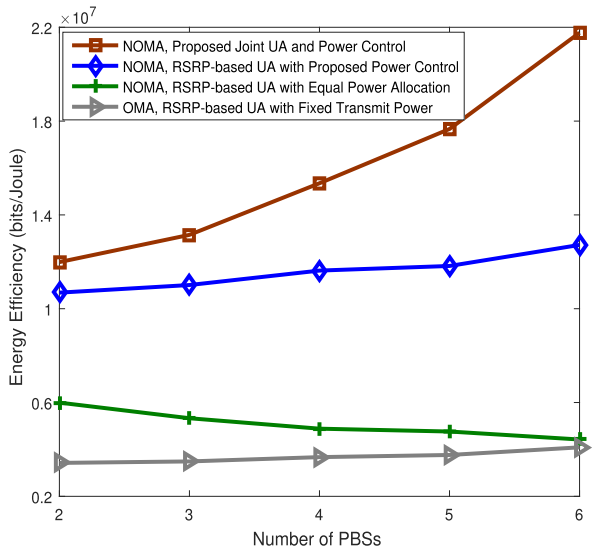

Fig. 8. Energy efficiency versus the number of PBSs for different joint UA and power allocation designs.

higher spectral efficiency. Additionally, when equal power allocation is adopted in NOMA HetNets with the conventional RSRP-based UA, energy efficiency decreases with increasing the number of UEs of the network, which can be explained by the fact that given the total transmit power of a BS, the transmit power allocated to the data-streams of the UEs with better channel condition reduces when more UEs are served simultaneously.

Fig. 8 shows the energy efficiency versus the number of PBSs with the number of UEs $N = 50$ and the energy transfer efficiency factor $\beta_{\mathcal{E}} = 0.9$. We set the minimum QoS as $\overline{\tau}_{\min} = 0.1$ bits/s/Hz and the amount of energy harvested by MBS and PBS as 37 dBm and 27 dBm, respectively. The proposed design outperforms the other cases. By using the proposed joint UA and power control with NOMA, the energy efficiency significantly increases with the PBS number, since the proposed design can obtain more BS densification gains. Again, the use of NOMA achieves better performance than OMA. For the case of RSRP-based UA with NOMA and equal power allocation, energy efficiency decreases with increasing the number of PBSs, because the inter-cell interference has a big adverse effect on the NOMA transmission [29].

VI. Conclusion and Future Work

This paper studied UA and power control in energy-cooperation aided two-tier HetNets with NOMA. A distributed UA algorithm was proposed based on the Lagrangian dual analysis, which does not require a central controller. Then, we proposed a joint UA and power control algorithm which achieves higher energy efficiency performance than the existing schemes. The proposed power control algorithm satisfies the KKT optimality conditions. Simulation results demonstrate the effectiveness of the proposed algorithms. The results showed that the proposed algorithm can efficiently coordinate the intra-cell and inter-cell interference and has the capability of exploiting the multiuser diversity and BS densification. The application of NOMA can achieve larger energy efficiency than OMA due to the higher spectral efficiency of NOMA.

To further extend this line of work, other UA optimization designs in multi-cell NOMA networks such as proportional fairness or max-min fairness would be of interest, and they are not trivial extensions since the optimization problems involved will be distinct. Moreover, imperfect CSI can have a substantial effect on outage probability and average data rate in NOMA networks, as analyzed in [47]. One of the challenges for optimization designs under imperfect CSI is that error propagation occurs since intra-cell interference cannot be perfectly canceled. Therefore, robust optimization designs need to be developed in multi-cell NOMA networks. In addition, the application of MIMO technology in NOMA networks is another important research area, which can significantly improve the performance gain [21]. In MIMO-NOMA networks, inter-user pair/group interference can deteriorate the performance, as analyzed in [21] and [48]. Therefore, how to mitigate the inter-user pair/group interference is crucial. Currently, UA and power control solutions in multi-cell MIMO-NOMA networks are not available, and more research efforts need to be made in this area.

References

[1] (2015). *5G-PPP 5G Vision*. [Online]. Available: https://5g-ppp.eu/wpcontent/uploads/2015/02/5G-Vision-Brochure-v1.pdf

[2] Cisco. (Mar. 2017). *Cisco Visual Networking Index: Global Mobile Data Traffic Forecast Update, 2016–2021 White Paper*. [Online]. Available: https://www.cisco.com/c/en/us/solutions/collateral/service-provider/visual-networking-index-vni/mobile-white-paper-c11-520862.html

[3] D. Jiang, P. Zhang, Z. Lv, and H. Song, "Energy-efficient multi-constraint routing algorithm with load balancing for smart city applications," *IEEE Internet Things J.*, vol. 3, no. 6, pp. 1437–1447, Dec. 2016.

[4] T. Han and N. Ansari, "Powering mobile networks with green energy," *IEEE Wireless Commun.*, vol. 21, no. 1, pp. 90–96, Feb. 2014.

[5] B. Gurakan, O. Ozel, J. Yang, and S. Ulukus, "Energy cooperation in energy harvesting two-way communications," in *Proc. IEEE Int. Conf. Commun.*, Jun. 2013, pp. 3126–3130.

[6] O. Ozel, K. Tutuncuoglu, J. Yang, S. Ulukus, and A. Yener, "Transmission with energy harvesting nodes in fading wireless channels: Optimal policies," *IEEE J. Sel. Areas Commun.*, vol. 29, no. 8, pp. 1732–1743, Sep. 2011.

[7] Y. Guo, J. Xu, L. Duan, and R. Zhang, "Joint energy and spectrum cooperation for cellular communication systems," *IEEE Trans. Commun.*, vol. 62, no. 10, pp. 3678–3691, Oct. 2014.

[8] B. Gurakan, O. Ozel, J. Yang, and S. Ulukus, "Energy cooperation in energy harvesting communications," *IEEE Trans. Commun.*, vol. 61, no. 12, pp. 4884–4898, Dec. 2013.

[9] B. Gurakan, O. Ozel, J. Yang, and S. Ulukus, "Two-way and multiple-access energy harvesting systems with energy cooperation," in *Proc. IEEE Asilomar Conf. Signals, Syst. Comput. (ASILOMAR)*, Nov. 2012, pp. 58–62.

[10] K. Tutuncuoglu and A. Yener, "Multiple access and two-way channels with energy harvesting and bi-directional energy cooperation," in *Proc. IEEE Inf. Theory Appl. Workshop (ITA)*, Feb. 2013, pp. 1–8.

[11] K. Tutuncuoglu and A. Yener, "Cooperative energy harvesting communications with relaying and energy sharing," in *Proc. IEEE Inf. Theory Workshop (ITW)*, Sep. 2013, pp. 1–5.

[12] D. Wang, P. Ren, Y. Wang, Q. Du, and L. Sun, "Energy cooperation for reciprocally-benefited spectrum access in cognitive radio networks," in *Proc. IEEE Global Conf. Signal Inf. Process. (GlobalSIP)*, Dec. 2014, pp. 1320–1324.

[13] Y.-K. Chia, S. Sun, and R. Zhang, "Energy cooperation in cellular networks with renewable powered base stations," *IEEE Trans. Wireless Commun.*, vol. 13, no. 12, pp. 6996–7010, Dec. 2014.

[14] J. Xu, L. Duan, and R. Zhang, "Cost-aware green cellular networks with energy and communication cooperation," *IEEE Commun. Mag.*, vol. 53, no. 5, pp. 257–263, May 2015.

[15] J. Xu and R. Zhang, "CoMP meets smart grid: A new communication and energy cooperation paradigm," *IEEE Trans. Veh. Technol.*, vol. 64, no. 6, pp. 2476–2488, Jun. 2015.

[16] S. Lakshminarayana, T. Q. S. Quek, and H. V. Poor, "Cooperation and storage tradeoffs in power grids with renewable energy resources," *IEEE J. Sel. Area Commun.*, vol. 32, no. 7, pp. 1386–1397, Jul. 2014.

[17] A. Jamalipour, T. Wada, and T. Yamazato, "A tutorial on multiple access technologies for beyond 3G mobile networks," *IEEE Commun. Mag.*, vol. 43, no. 2, pp. 110–117, Feb. 2005.

[18] S. M. R. Islam, N. Avazov, O. A. Dobre, and K.-S. Kwak, "Power-domain non-orthogonal multiple access (NOMA) in 5G systems: Potentials and challenges," *IEEE Commun. Surveys Tuts.*, vol. 19, no. 2, pp. 721–742, 2nd Quart., 2017.

[19] Y. Saito, Y. Kishiyama, A. Benjebbour, T. Nakamura, A. Li, and K. Higuchi, "Non-orthogonal multiple access (NOMA) for cellular future radio access," in *Proc. IEEE 77th Veh. Tech. Conf. (VTC Spring)*, Jun. 2013, pp. 1–5.

[20] L. Dai, B. Wang, Y. Yuan, S. Han, C.-L. I, and Z. Wang, "Non-orthogonal multiple access for 5G: Solutions, challenges, opportunities, and future research trends," *IEEE Commun. Mag.*, vol. 53, no. 9, pp. 74–81, Sep. 2015.

[21] Z. Ding, F. Adachi, and H. V. Poor, "The application of MIMO to non-orthogonal multiple access," *IEEE Trans. Wireless Commun.*, vol. 15, no. 1, pp. 537–552, Jan. 2016.

[22] Y. Zhang, H.-M. Wang, T.-X. Zheng, and Q. Yang, "Energy-efficient transmission design in non-orthogonal multiple access," *IEEE Trans. Veh. Technol.*, vol. 66, no. 3, pp. 2852–2857, Mar. 2017.

[23] Z. Yang, Z. Ding, P. Fan, and N. Al-Dhahir, "A general power allocation scheme to guarantee quality of service in downlink and uplink NOMA systems," *IEEE Trans. Wireless Commun.*, vol. 15, no. 11, pp. 7244–7257, Nov. 2016.

[24] J. Cui, Z. Ding, and P. Fan, "A novel power allocation scheme under outage constraints in NOMA systems," *IEEE Signal Process. Lett.*, vol. 23, no. 9, pp. 1226–1230, Sep. 2016.

[25] F. Fang, H. Zhang, J. Cheng, and V. C. M. Leung, "Energy-efficient resource allocation for downlink non-orthogonal multiple access network," *IEEE Trans. Commun.*, vol. 64, no. 9, pp. 3722–3732, Sep. 2016.

[26] Z. Wei, D. W. K. Ng, and J. Yuan, "Power-efficient resource allocation for MC-NOMA with statistical channel state information," in *Proc. IEEE Global Commun. Conf. (GLOBECOM)*, Dec. 2016, pp. 1–7.

[27] Y. Sun, D. W. K. Ng, Z. Ding, and R. Schober, "Optimal joint power and subcarrier allocation for MC-NOMA systems," in *Proc. IEEE Global Commun. Conf. (GLOBECOM)*, Dec. 2016, pp. 1–6.

[28] D. Liu *et al.*, "User association in 5G networks: A survey and an outlook," *IEEE Commun. Surveys Tuts.*, vol. 18, no. 2, pp. 1018–1044, 2nd Quart., 2016.

[29] W. Shin, M. Vaezi, B. Lee, D. J. Love, J. Lee, and H. V. Poor. (Nov. 2016). "Non-orthogonal multiple access in multi-cell networks: Theory, performance, and practical challenges." [Online]. Available: https://arxiv.org/abs/1611.01607

[30] Y. Li, M. Sheng, Y. Sun, and Y. Shi, "Joint optimization of BS operation, user association, subcarrier assignment, and power allocation for energy-efficient hetnets," *IEEE J. Sel. Areas Commun.*, vol. 34, no. 12, pp. 3339–3353, Dec. 2016.

[31] G. Ye, H. Zhang, H. Liu, J. Cheng, and V. C. M. Leung, "Energy efficient joint user association and power allocation in a two-tier heterogeneous network," in *Proc. IEEE Global Commun. Conf. (GLOBECOM)*, Dec. 2016, pp. 1–5.

[32] B. Di, L. Song, and Y. Li, "Sub-channel assignment, power allocation, and user scheduling for non-orthogonal multiple access networks," *IEEE Trans. Wireless Commun.*, vol. 15, no. 11, pp. 7686–7698, Nov. 2016.

[33] K. Son, H. Kim, Y. Yi, and B. Krishnamachari, "Base station operation and user association mechanisms for energy-delay tradeoffs in green cellular networks," *IEEE J. Sel. Areas Commun.*, vol. 29, no. 8, pp. 1525–1536, Sep. 2011.

[34] D. Liu, Y. Chen, K. K. Chai, T. Zhang, and M. Elkashlan, "Two-dimensional optimization on user association and green energy allocation for HetNets with hybrid energy sources," *IEEE Trans. Commun.*, vol. 63, no. 11, pp. 4111–4124, Nov. 2015.

[35] D. Tse and P. Viswanath, *Fundamentals of Wireless Communication*. Cambridge, U.K.: Cambridge Univ. Press, 2005.

[36] J. G. Andrews *et al.*, "What will 5G be?" *IEEE J. Sel. Areas Commun.*, vol. 32, no. 6, pp. 1065–1082, Jun. 2014.

[37] S. Boyd and A. Mutapcic, *Subgradient Methods*. Stanford, CA, USA: Stanford Univ. Press, 2008.

[38] K. Yasuda, L. Hu, and Y. Yin, "A grouping genetic algorithm for the multi-objective cell formation problem," *Int. J. Prod. Res.*, vol. 43, no. 4, pp. 829–853, Feb. 2005.

[39] D. E. Goldberg and K. Deb, *A Comparative Analysis of Selection Schemes Used in Genetic Algorithms*. San Mateo, CA, USA: Morgan Kaufmann, 1991.

[40] M. Grant and S. Boyd. (Apr. 2011). *CVX: Matlab Software for Disciplined Convex Programming, Version 1.21*. [Online]. Available: http://cvxr.com/cvx/

[41] Z. Han, D. Niyato, W. Saad, T. Başar, and A. Hjøungnes, *Game Theory in Wireless and Communication Networks: Theory, Models, and Applications*. Cambridge, U.K.: Cambridge Univ. Press, 2012.

[42] M. Kobayashi and G. Caire, "An iterative water-filling algorithm for maximum weighted sum-rate of Gaussian MIMO-BC," *IEEE J. Sel. Areas Commun.*, vol. 24, no. 8, pp. 1640–1646, Aug. 2006.

[43] A. Ghosh *et al.*, "Heterogeneous cellular networks: From theory to practice," *IEEE Commun. Mag.*, vol. 50, no. 6, pp. 54–64, Jun. 2012.

[44] S. Zhang, N. Zhang, S. Zhou, J. Gong, Z. Niu, and X. S. Shen, "Energy-aware traffic offloading for green heterogeneous networks," *IEEE J. Sel. Areas Commun.*, vol. 34, no. 5, pp. 1116–1129, May 2016.

[45] T. Han and N. Ansari, "Green-energy aware and latency aware user associations in heterogeneous cellular networks," in *Proc. IEEE Global Commun. Conf. (GLOBECOM)*, Dec. 2013, pp. 4946–4951.

[46] D. W. K. Ng, E. S. Lo, and R. Schober, "Energy-efficient resource allocation in OFDMA systems with large numbers of base station antennas," *IEEE Trans. Wireless Commun.*, vol. 11, no. 9, pp. 3292–3304, Sep. 2012.

[47] Z. Yang, Z. Ding, P. Fan, and G. K. Karagiannidis, "On the performance of non-orthogonal multiple access systems with partial channel information," *IEEE Trans. Commun.*, vol. 64, no. 2, pp. 654–667, Feb. 2016.

[48] Z. Ding, R. Schober, and H. V. Poor, "A general MIMO framework for NOMA downlink and uplink transmission based on signal alignment," *IEEE Trans. Wireless Commun.*, vol. 15, no. 6, pp. 4438–4454, Jun. 2016.

Bingyu Xu received the double B.Sc. degrees in telecommunications engineering with management from the Beijing University of Posts and Telecommunications, China, and the Queen Mary University of London, London, U.K., in 2014, where she is currently pursuing the Ph.D. degree in electronic engineering. Her current research interests include radio resource allocation optimization in HetNets, cooperative wireless networking, millimeter wave, and smart energy systems.

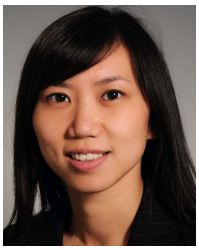

Yue Chen (S'02–M'03–SM'15) received the Ph.D. degree from the Queen Mary University of London, London, U.K., in 2003. She is currently a Professor of Telecommunications Engineering with the School of Electronic Engineering and Computer Science, Queen Mary University of London. Her current research interests include intelligent radio resource management for wireless networks, MAC and network layer protocol design, cognitive and cooperative wireless networking, HetNets, smart energy systems, and Internet of Things.

Jesús Requena Carrión (M'08) received the degree in telecommunication engineering degree in 2003 and the Ph.D. degree in multimedia and telecommunications engineering from the Carlos III University of Madrid in 2008. He is currently a Lecturer (Assistant Professor) with the School of Electronic Engineering and Computer Science, Queen Mary University of London. His main research interests include statistical signal processing and computer modeling and simulation of complex systems.

Tiankui Zhang (M'10–SM'15) received the M.S. degree in communication engineering from the Beijing University of Posts and Telecommunications (BUPT) in 2003 and the Ph.D. degree in information and communication engineering from BUPT in 2008. He is currently an Associate Professor with the School of Information and Communication Engineering, BUPT. He has authored over 100 papers, including journal papers on the IEEE JOURNAL ON SELECTED AREAS IN COMMUNICATIONS, the IEEE TRANSACTION ON COMMUNICATIONS, the IEEE COMMUNICATION LETTERS, and conference papers, such as the IEEE GLOBECOM and the IEEE ICC. His research interests are in wireless communication networking, green wireless networking, signal processing for wireless communications, and content centric wireless networks.